25p

[redacted]

FM TELEMETRY AND FREE-FLIGHT TECHNIQUES FOR AERODYNAMIC MEASUREMENTS IN CONVENTIONAL WIND TUNNELS

by

TMX 51648

Ronald J. Hruby and John B. McDevitt

National Aeronautics and Space Administration
Ames Research Center
Moffett Field, California

Presented at Twenty-First Semi-Annual Meeting
of the Supersonic Tunnel Association

Princeton, New Jersey
April 6-7, 1964

[redacted]

INTRODUCTION

Aerodynamic data obtained in conventional wind tunnels are subject to possible interference effects from the model-support system. Estimates of support-interference effects become uncertain at hypersonic speeds, especially in studies of base flows or flows over afterbodies on shapes such as the Apollo capsule. Dayman at JPL (ref. 1) has successfully utilized a free-flight technique in conventional wind tunnels to obtain force and moment data free of support-interference effects. A natural extension of this technique would be the incorporation of a telemetry system so that surface pressures, convective heating, etc., could also be measured in the absence of support-interference effects. The development of such a telemetry system was successfully completed recently at the Ames Research Center and descriptions of this sytems and the associated free-flight technique are presented herein.

The free-flight motion of the test model is achieved by the use of a simple pneumatic launching device placed in the tunnel downstream of the test section. The launch device propels the test model upstream with sufficient velocity that its upstream motion terminates near the upstream edge of the test-section viewing windows. High-speed motion pictures of the model provide an extensive photographic record which is evaluated in the same manner as in ballistic-range testing. An important advantage of this technique, compared to the usual ballistic-range method, is that the acceleration forces on the models are relatively small. This, of course, greatly enhances the possibility of designing accurate and reliable telemetering devices.

In this paper a description of the FM telemetry system is presented first, followed by a discussion of the free-flight technique. Base-pressure measurements for a 15° half-angle cone in free flight at hypersonic speeds are then presented to illustrate the practical application of these methods in aerodynamic testing.

FM TELEMETRY SYSTEM

The relatively small accelerations encountered during launch and free-flight motion of the test model permit use of state-of-the-art circuitry and components in the telemetry system. Nevertheless, considerable care must be exercised in the choice of electrical components to insure stability of the system, and the use of a wide FM bandwidth is necessary to eliminate systematic errors as much as possible.

An attempt has been made in the past (see ref. 2) to measure stagnation pressures by radiotelemetry from a model magnetically supported in a wind tunnel. It was found that large temperature

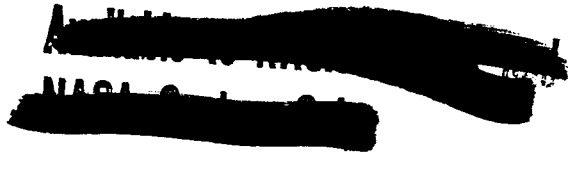

interactions with the telemetry center frequency could arise and methods for reducing the temperature effects were suggested. In the present telemetry system possible temperature interaction effects were effectively eliminated by use of a temperature compensating circuit in the telemeter and by mounting the telemeter in plastic test models so as to thermally insulate the electronic components from the surrounding hypersonic flow field during wind-tunnel testing.

The basic components of the telemetry system are shown in figure 1. The 1.5-milliwatt VHF telemeter is implanted in the aerodynamic test vehicle, as shown in figure 2. It consists of a miniature transistorized oscillator with a capacitance-type pressure transducer incorporated in the circuit such that the oscillation frequency is controlled by the differential pressure within the transducer. The receiving system utilizes a VHF antenna (receiving coil) mounted directly on the test-section viewing window. The antenna is coupled through a VHF preamp to an FM receiver. The demodulated signal drives a recording oscillograph and, if desired, an analog-to-digital converter and digital data recorder. A description of the various components of the system follows.

Telemeter

The telemeter is a VHF common-emitter oscillator (see discussion in ref. 3), frequency modulated by means of a variable-capacitance pressure cell. The oscillator circuit and pressure transducer were designed for use with an FM receiver having a tuning range of 105 - 140 mc and a maximum I.F. bandwidth of ±0.8 mc.

Details of the oscillator circuit and its mechanical layout are shown in figure 3. The complete telemetry unit is mounted on a 7/8-inch-diameter printed-circuit wafer. The two-turn oscillator coil is a printed-circuit element located on the outside perimeter of both the front and back faces of the printed-circuit wafer. The feedback element consists of a printed-circuit secondary coil located inside the oscillator coil and provides a four-to-one reduction in signal. The transistor used in the oscillator circuit (Fairchild FSP-293-1, 2N709, or equivalent) provides a gain bandwidth product of 4×10^8 cps in this application. A common-emitter circuit is used because it provides a more stable operation when the operating frequency is near the 180° phase shift frequency of the transistor (see discussion in ref. 3). A transformer feedback circuit was utilized because capacitor C_1 corrects the feedback phase shift arising from the transistor VHF α characteristics. Temperature stability is provided by the thermistor T. Capacitor C_2 provides a low impedance path across the batteries to eliminate any reactivity they might introduce into the circuit. Resistor R adjusts the quiescent operating point of the

circuit. The best operation was obtained with a quiescent collector current $i_{C_{D.C.}}$ of about 0.5 ma. A somewhat greater value of $i_{C_{D.C.}}$ was used to minimize possible variations in circuit performance due to transistor characteristics.

The nominal value of the transducer capacitance (no differential pressure) is 7μμf. With the coil and circuit of figure 3, this gives a nominal operating frequency of 117 mc. However, manufacturing tolerances of the printed-circuit wafer and of the pressure transducer cause the nominal center frequency to fall in the range 117 ±12 mc. The capacitance-versus-pressure slope of each transducer combined with the available bandwidth of the FM receiver determines the usable pressure range of each transducer. Generally, the pressure differential which would give the maximum allowable frequency modulation is a very small part of the linear mechanical range of the pressure cell. In the present case the range of the transducer capacitance is ±0.096μμf for the available bandwidth of ±0.8 mc.

Antenna and VHF Preamplifier

The oscillator coil axis is oriented parallel to the center line of the wind tunnel. The field pattern within the tunnel corresponds to a cylindrical TE_{01} mode below cutoff (ref. 4). The antenna (receiving coil) is oriented to provide maximum coupling to the tunnel-wall-equivalent-surface current. Energy coupled to the receiving coil develops a voltage across the 50Ω cable-matching resistor and drives a preamplifier with high input impedance. The preamplifier output is matched to a 50Ω coaxial cable which in turn drives the high impedance RF input of the FM receiver.

The VHF preamplifier was used to allow flexibility in the RF signal handling. A circuit diagram is shown in figure 4. If two receiving coils are used (e.g., one on each of the test section windows) the preamplifier provides rejection of common-mode extraneous signals. This differential connection of receiving coils and preamplifier provided a 6 db to 15 db improvement in signal-to-noise ratio. Inductance L_O provides the common-mode rejection at VHF frequencies. Transistor Q_3 adjusts the sum of collector currents of transistors Q_1 and Q_2 to be 20 ma; hence, the output voltage has a source impedance given by resistor R_3, or 50Ω. The coupling capacitors were Corning Glass VHF units. The ability of this amplifier to operate satisfactorily in the differential mode is dependent upon careful shielding between the different stages which is provided by the use of separate input and output compartments. These compartments are shown in figure 5(a). The battery compartment and constant current stage are shown in figure 5(b). Two essential features of the preamplifier (ref. 5) are its high input impedance (to prevent loading of the receiving coil circuit) and its

constant 50 ohm output impedance (to prevent signal distortion due to output cable impedance).

FM Receiver and Data Recorder

The FM receiver used in this system is the Defense Electronics, Inc., TMR-5A Receiver with a tuning range of 105-140 mc and an I.F. bandwidth of 1.6 mc. The dynamic range of the receiver is 2 microvolts to 20,000 microvolts.

A classical FM system would have utilized a bandwidth which was minimum for the maximum information rate. For example, a signal having an information content of 1 kc would be transmitted to a receiver having an FM bandwidth of 0 to about 5 kc or 10 kc. However, the present telemetry system was developed for a single enclosed channel where possible errors (ref. 6) in signal might arise from oscillator detuning, drift, frequency changes due to launch-flight stresses, and the proximity of large metallic surfaces. These types of errors were minimized by using a wide-band FM signal. For the deviation ratios actually used, it was observed that the cumulative frequency errors at the receiver output were not greater than 2 kc during any specific test.

The direct-coupled output of the receiver detector drives a recording oscillograph preamplifier (see fig. 1) which provides both the proper input impedance (for galvanometer damping) and voltage range for the Consolidated Electrodynamic Recording Oscillograph. A resistor-matching network was used to prevent overload of the Beckman Digital data recorder and maintain proper voltage and source impedance to the CEC oscillograph. This part of the system is also shown in figure 1. Although the pressure transducer with its inlet tube was found to be capable of a frequency response dynamic range greater than 1 kc, for practical reasons, a galvanometer with a flat response to 1 kc was used. The data were simultaneously recorded on the Beckman Data Recorder, which records the data in binary coded decimal form on magnetic tape, and the CEC oscillograph. The time required by the Beckman to record one datum point was about 0.4 millisecond which was adequate to provide data at frequencies to 1 kilocycle/sec. The recorded base-pressure data were synchronized with the photographs of the model by means of a timing pulse which was recorded simultaneously on the photographs, the magnetic tape, and the CEC oscillograph.

FREE-FLIGHT TESTING TECHNIQUE

The first attempts to obtain free-flight data in conventional tunnels involved suspension of the test models on wires which were broken at the appropriate time to release the model into a free-flight trajectory through the test section. The use of an air gun on the tunnel center line to propel the test models upstream into the viewing area has been successfully used, as previously mentioned, by Dayman (ref. 1). The latter method, when it can be used, has the advantage of giving at least twice the amount of data of the wire supported system since the model can be viewed in both upstream and downstream traverses of the viewing area. The pneumatic launching technique was used in the development of the present telemetry system and a brief description follows.

A schematic of the Ames 14-Inch Helium Tunnel and pneumatic model launcher are shown in figures 6 and 7. The launch device consists of a piston and rod on which the model is mounted (fig. 7). The piston is contained in a tube and "firing" of the test model is accomplished by release of the restraining pin. The upstream side of the piston is vented to the tunnel static pressure (much less than $\bar{p}_1$) while the driving pressure, $\bar{p}_1$, is set at a predetermined value such that the launch velocity, $\bar{V}_1$, of the model results in an upstream trajectory which terminates near the upstream edge of the viewing window (see fig. 8).

The launch velocity $\bar{V}_1$ (ft/sec) to give the trajectory indicated in figure 8 and the time in seconds to travel the distance $\bar{s}_1$ (ft) is calculated from the relationships

$$V_1 = \sqrt{\frac{2D\bar{s}_1}{m_m}} \tag{1}$$

$$t = \sqrt{\frac{2m_m\bar{s}_1}{D}} \tag{2}$$

where

D aerodynamic drag of model, lb

m_m mass of test model, slugs

The time, t, is considered first and the maximum value is used which is the time for a free-falling object to travel the vertical height $\bar{h}_1$ (see fig. 8). This defines the proper ratio between model mass and aerodynamic drag. The required launch velocity $\bar{V}_1$ can then be calculated from equation (1).

The initial free-flight velocity, $\bar{V}_1$, is relatively small (usually less than 100 fps) and the required reservoir pressure $\bar{p}_1$ to achieve this velocity can readily be estimated by assuming that the driving gas remains in equilibrium and that the expansion is isentropic. It is also convenient to assume $\bar{p}_2 = 0$ (see fig. 7) since the upstream side of the launch tube is vented to tunnel static pressure. The initial velocity at launch is then related to the driving pressure $\bar{p}_1$ by the approximate relationship

$$\bar{V}_1^2 = \frac{2\bar{l}_2}{m_m + m_p}\left[\bar{A}_p\bar{p}_1 f\left(\gamma, \frac{\bar{l}_2}{\bar{l}_1}\right) - (D + D_f)\right] \tag{3}$$

and by use of equation (1) a convenient expression for estimating the reservoir pressure is obtained

$$\bar{p}_1 = \frac{D\left\{1 + (\bar{s}_1/\bar{l}_2)[1 + (m_p/m_m)]\right\} + D_f}{\bar{A}_p f[\gamma, (\bar{l}_2/\bar{l}_1)]} \tag{4}$$

where (see figs. 7 and 8)

$\bar{l}_1$ length of reservoir, ft

$\bar{l}_2$ piston stroke, ft

$\bar{p}_1$ reservoir pressure, lb/ft^2

$\bar{A}_p$ cross-sectional area of piston, ft^2

m_p mass of piston ensemble, slugs

D_f friction drag of piston, lb

and the energy function is given by

$$f\left(\gamma, \frac{\bar{l}_2}{\bar{l}_1}\right) = \frac{1}{(\bar{l}_2/\bar{l}_1)(\gamma - 1)}\left\{1 - \frac{1}{[1 + (\bar{l}_2/\bar{l}_1)]^{\gamma-1}}\right\} \tag{5}$$

where γ is the specific-heat ratio. The increase in energy available by increasing the length of the reservoir, $\bar{l}_1$, for a given piston stroke, $\bar{l}_2$, is indicated in figure 9. It is evident that little is to be gained by using a large value of $\bar{l}_1$. In the present application a piston diameter of 1 inch, a stroke of $\bar{l}_2 = 6$ in., and reservoir length of $\bar{l}_1 = 12$ in. were used.

TEST RESULTS

The first application of the present telemetry system involved the measurement of base pressures on cones and afterbody pressures on the current Apollo configuration. The test results for a 15° half-angle cone are presented here as an illustrative example of the present telemetry technique.

Model Details

A schematic drawing of the test model (15° half-angle cone) and support system on which the model rests until launched is presented in figure 10. The model and model holder were constructed entirely of nonmetallic material (plastic) so that the telemeter center frequency would not be significantly affected by either the model or the holder. The plastic model construction also served to thermally insulate the telemeter electronic components from the surrounding hypersonic flow field during wind-tunnel testing and thus minimize temperature interaction effects.

Since a differential-type pressure transducer was used, provision had to be made for applying a known pressure level to the "reference" side of the pressure cell. The inside cavity of the model, where the telemeter and pressure transducer are located, serves as the reference-pressure chamber. A hypodermic needle (see fig. 10), inserted through a small rubber disk at the model base, is used to provide known changes in the reference pressure during calibration of the system and to monitor the reference pressure immediately prior to launching of the model. The needle is pulled out of the model during the initial portion of the launch.

Extensive tests were made in order to determine the accuracy and response time of the system. By using hypodermic needles having inside diameters greater than 0.03 inch and applying reference pressures greater than 2000 microns (greater than about 0.04 psi) the reference pressure was subject to errors less than ±50 microns. For a step pressure impulse applied at the base-pressure orifice the time required for the telemetry signal to exceed 90 percent of the new steady-state value was approximately 0.6 millisecond.

For this particular test model, the differential pressure cell was designed so that a 0.15-psi differential loading resulted in a 0.6 megacycle shift in center frequency of the telemeter. The calibration of the telemetry system is shown in figure 11, and it can be seen that the system is linear for loadings up to about 0.05 psi. The battery life of the telemeter oscillator was about 20 hours, which was more than adequate for repeated preflight calibrations and tests of the model.

Base Pressure Measurements

The test of the cone model with base-pressure telemetry was made for a free-stream Mach number of 10.7 and free-stream static pressure of 0.046 psi. For this tunnel the flow can be brought to the desired test conditions in about 5 seconds. A timing device is then used to initiate the test equipment in the proper sequence. The high-speed camera that records the motion of the test model in the viewing area is started first, then the data recording equipment, and, finally, launching of the model is initiated. Reference time marks are used to synchronize the motion pictures with the telemetry data recorder in order that proper interpretation of the data can be made.

The possibility of changes in model temperature affecting the telemeter frequency was carefully checked. A thermocouple was placed in the reference pressure cavity of the model near the telemeter package. The model was sting mounted (not launched) and the temperature monitored for a tunnel run of 20 seconds. In this time interval, which is considerably longer than that required for a typical free-flight test, the temperature at the telemeter did not change.

During launch, and during the free-flight trajectory in the tunnel hypersonic flow, the test model is subject to appreciable, but not excessive, acceleration forces. The test model, with the base-pressure orifice closed, was launched into still air in order to assess possible g effects. The recorded telemetry data during launch indicated that the acceleration force did not noticeably change the telemetry center frequency.

The high-speed data recording of the base-pressure telemetry reading in free flight is reproduced in figure 12. With the model near the launcher, point A of figure 12, the base-pressure reading is quite high due to interference effects between the model wake and the model-holder portion of the launcher. From point B to C, for which the time interval is about 80 milliseconds, the telemetry signal is constant and the pressure value is 0.017 psi. At point C, the model has fallen into the boundary layer near the tunnel walls and the near proximity of the telemeter oscillator to the tunnel walls results in an abrupt shift in telemetry frequency. Shortly thereafter the signal is lost.

The ratio of model base pressure to free-stream static pressure is presented in figure 13 for this free-flight test and for prior tests of the same model mounted on various sizes of support stings. It is clearly evident that sting interference effects persist even for very small sting sizes. For example, when the cross-sectional area of the sting is only 4 percent of the model base area ($D_s/D_m = 0.2$), the base pressure is about 50 percent higher than that measured in free flight.

CONCLUDING REMARKS

The present FM telemetry system is currently being used at the Ames Research Center to measure base pressures in free-flight on conical test models and afterbody pressures on entry vehicles such as the Apollo configuration. The response time of the pressure sensing system has been found to be less than 1 millisecond in most applications. Experience to date with this system has indicated that the uncertainties in the pressure measurements are less than 2 percent for pressure readings greater than about 0.1 psi and less than 100 microns (0.002 psi) for pressure readings less than 0.1 psi. The pneumatic model launching method used provided relatively repeatable free-flight trajectories in which the test model was free of support interference effects for time intervals approaching 100 milliseconds.

The successful development of the present telemetry system was due partly to the careful choice of components so as to insure stability in both the telemeter and the receiving equipment, and to the use of a wide bandwidth FM system. In addition, possible temperature interaction effects were effectively eliminated by use of a temperature compensating circuit in the telemeter and by mounting the telemeter in plastic test models so as to thermally insulate the electronic components from the surrounding hypersonic flow field during wind-tunnel testing.

Modifications to the present system are being made in order to permit use of the free-flight telemetry technique in shock tunnels. The development of a telemetry system for measuring convective heating on models in free flight is also currently under way.

REFERENCES

1. Dayman, Bain, Jr.: Simplified Free-Flight Testing in a Conventional Wind Tunnel. JPL Tech. Rep. 32-346, 1962.

2. Clemens, P. L.: Radio Telemetry of Stagnation Pressure from a Wind Tunnel Model Magnetically Supported in Supersonic Flow. AEDC TDR-62-141, 1962.

3. Hunter, L. P.: Handbook of Semi-Conductor Electronics. Second ed., McGraw-Hill Book Co., Inc., 1962, pp. 14-1, 14-23.

4. Ramo-Whinnery: Fields and Waves in Modern Radio. Second ed., John Wiley and Sons, Inc., 1956, pp. 177-415.

5. Langford-Smith: Radiotron Designer's Handbook. Fourth ed., RCA, 1952, pp. 450-453.

6. Terman, F. E.: Radio Engineer's Handbook. McGraw-Hill Book Co., Inc., 1943.

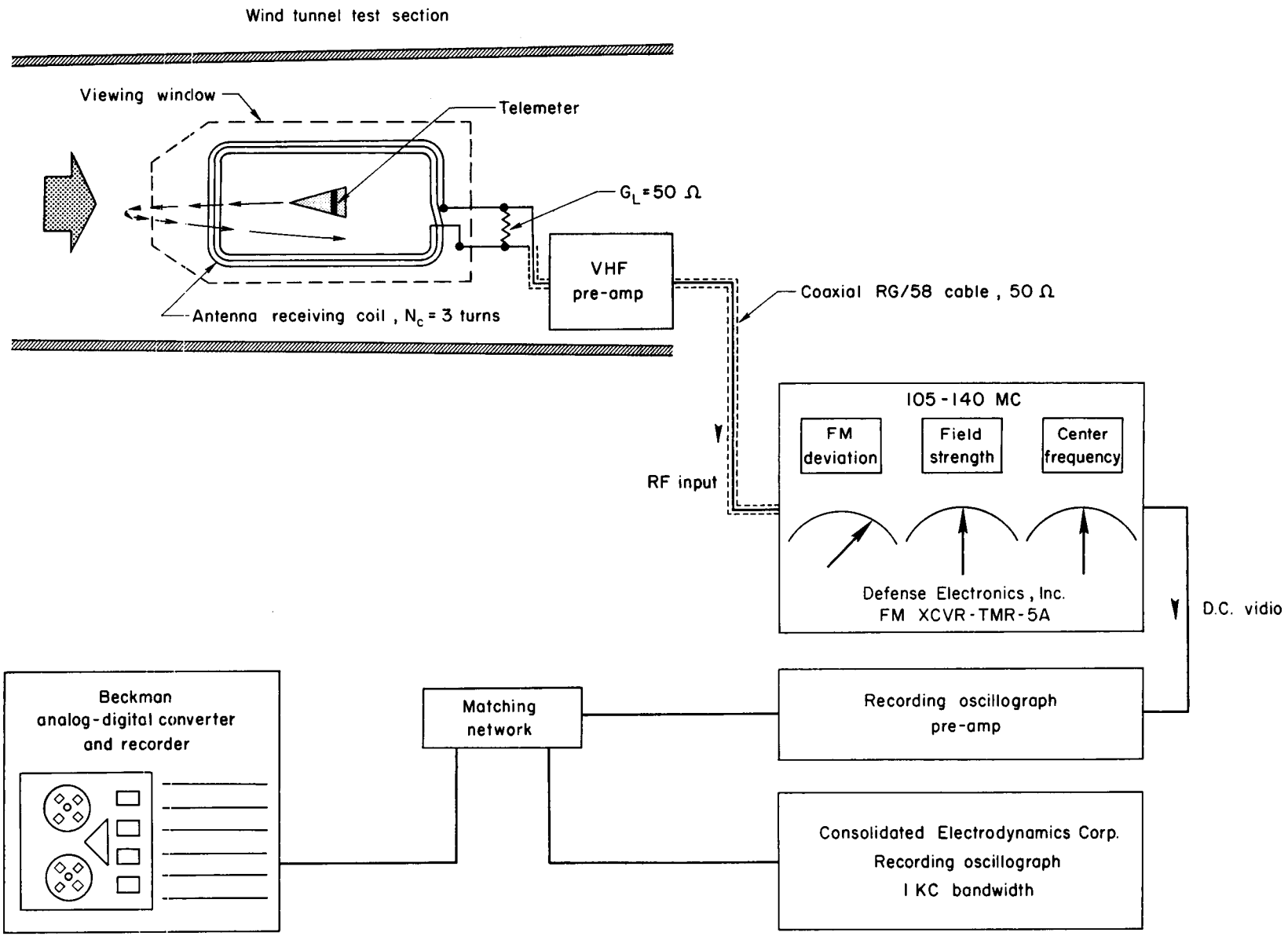

Figure 1.- FM telemetry system.

NATIONAL AERONAUTICS AND SPACE ADMINISTRATION
AMES RESEARCH CENTER, MOFFETT FIELD, CALIFORNIA

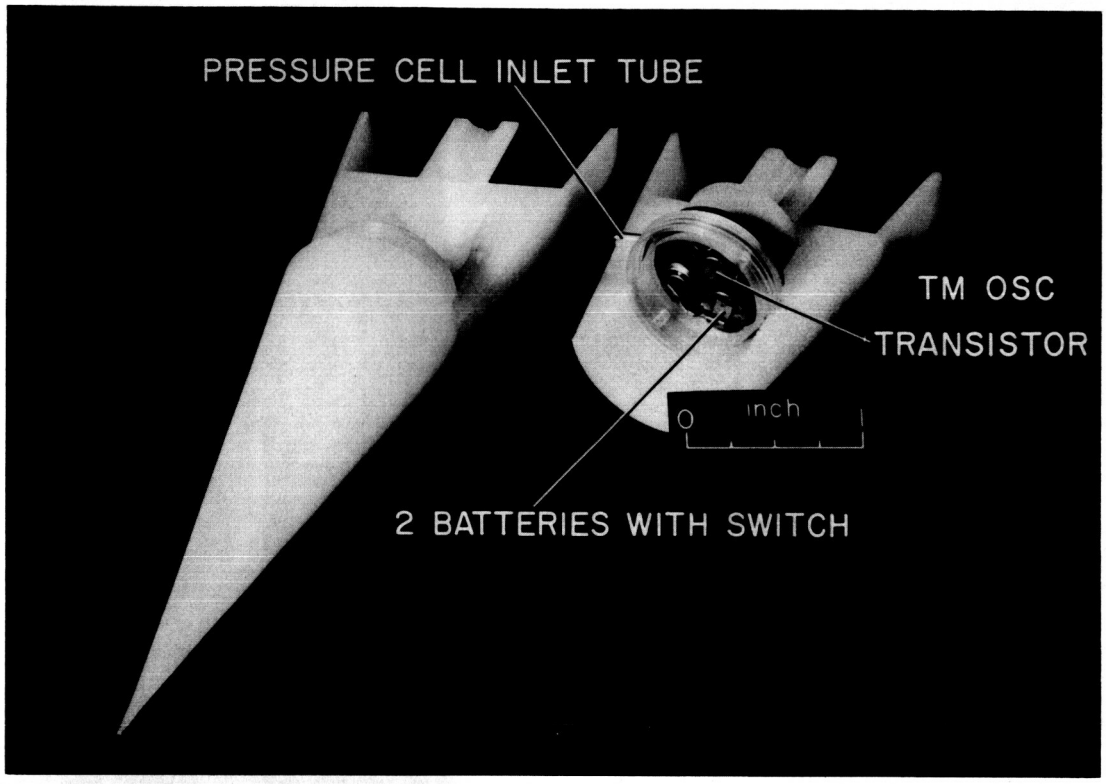

A-32043.1

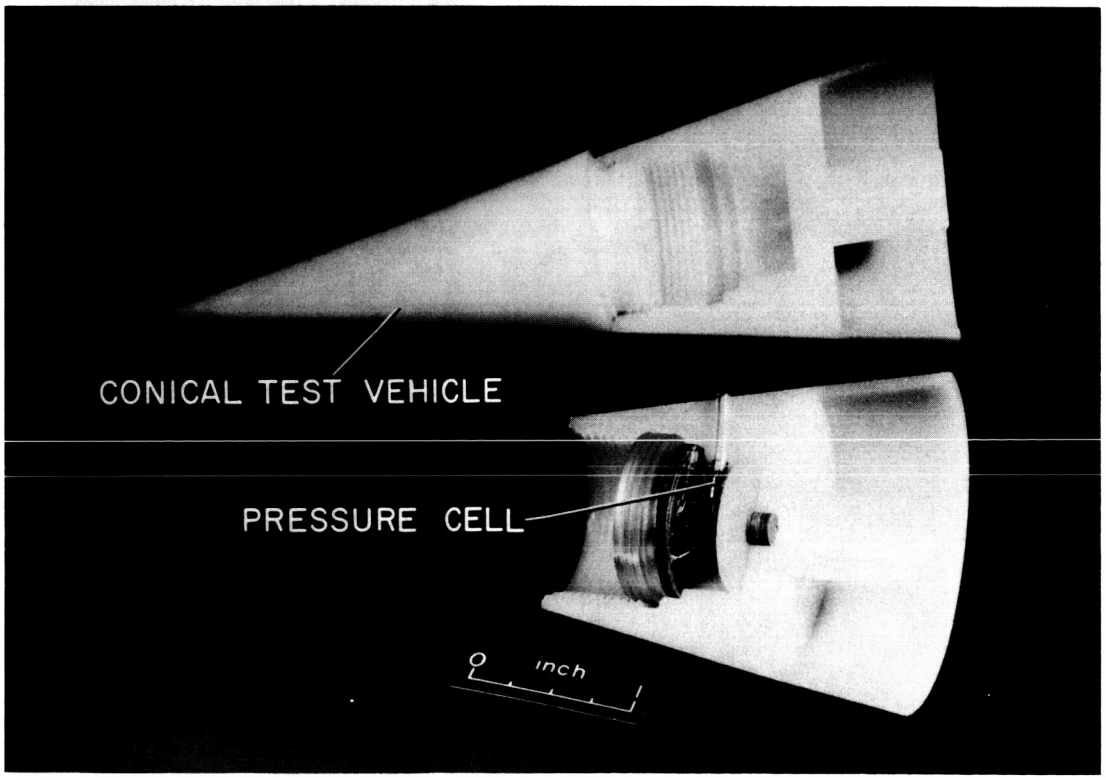

A-32044.1

Figure 2.- Photographs of typical model with telemeter.

NATIONAL AERONAUTICS AND SPACE ADMINISTRATION
AMES RESEARCH CENTER, MOFFETT FIELD, CALIFORNIA

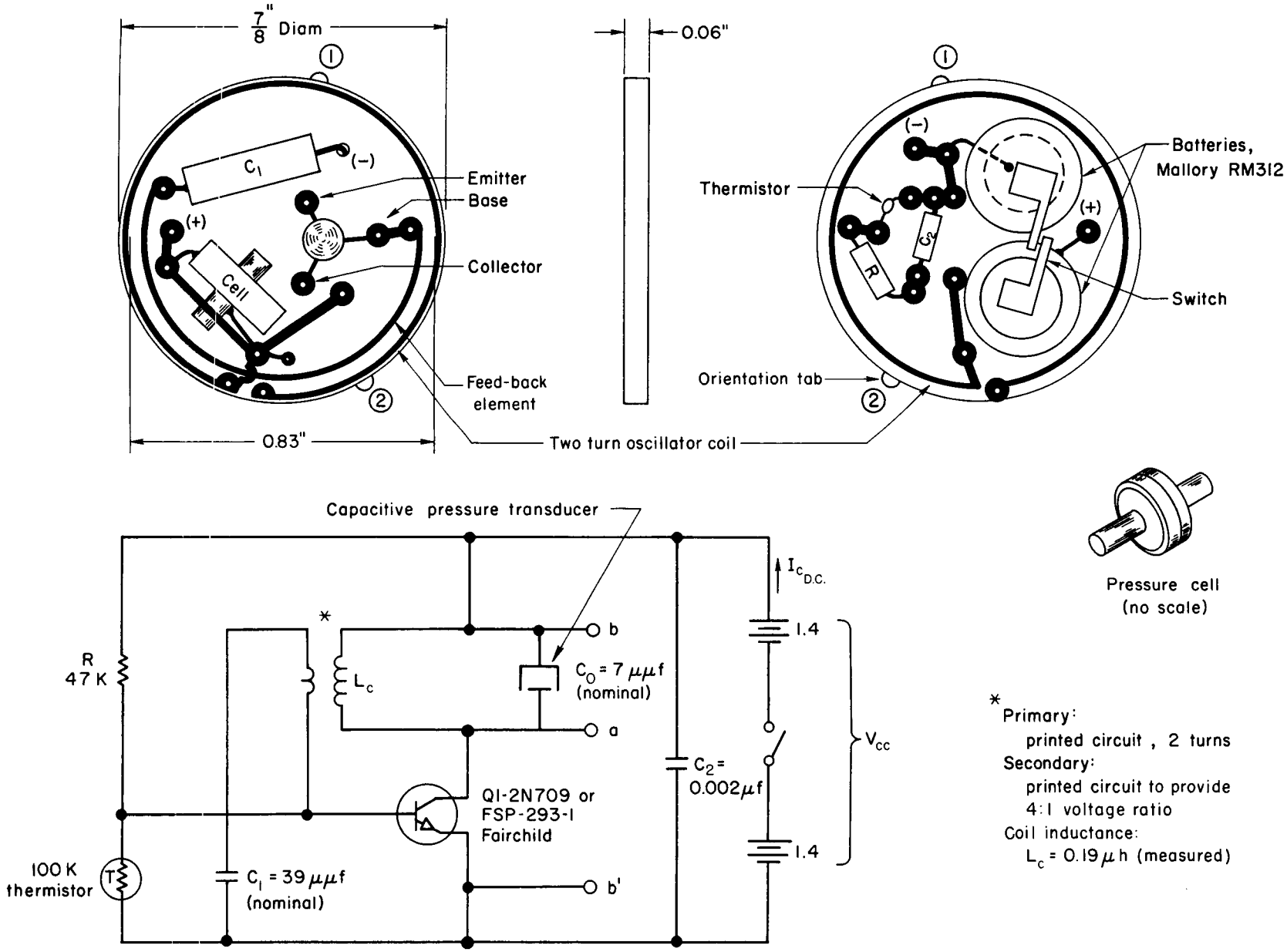

Figure 3.- Telemeter details.

NATIONAL AERONAUTICS AND SPACE ADMINISTRATION
AMES RESEARCH CENTER, MOFFETT FIELD, CALIFORNIA

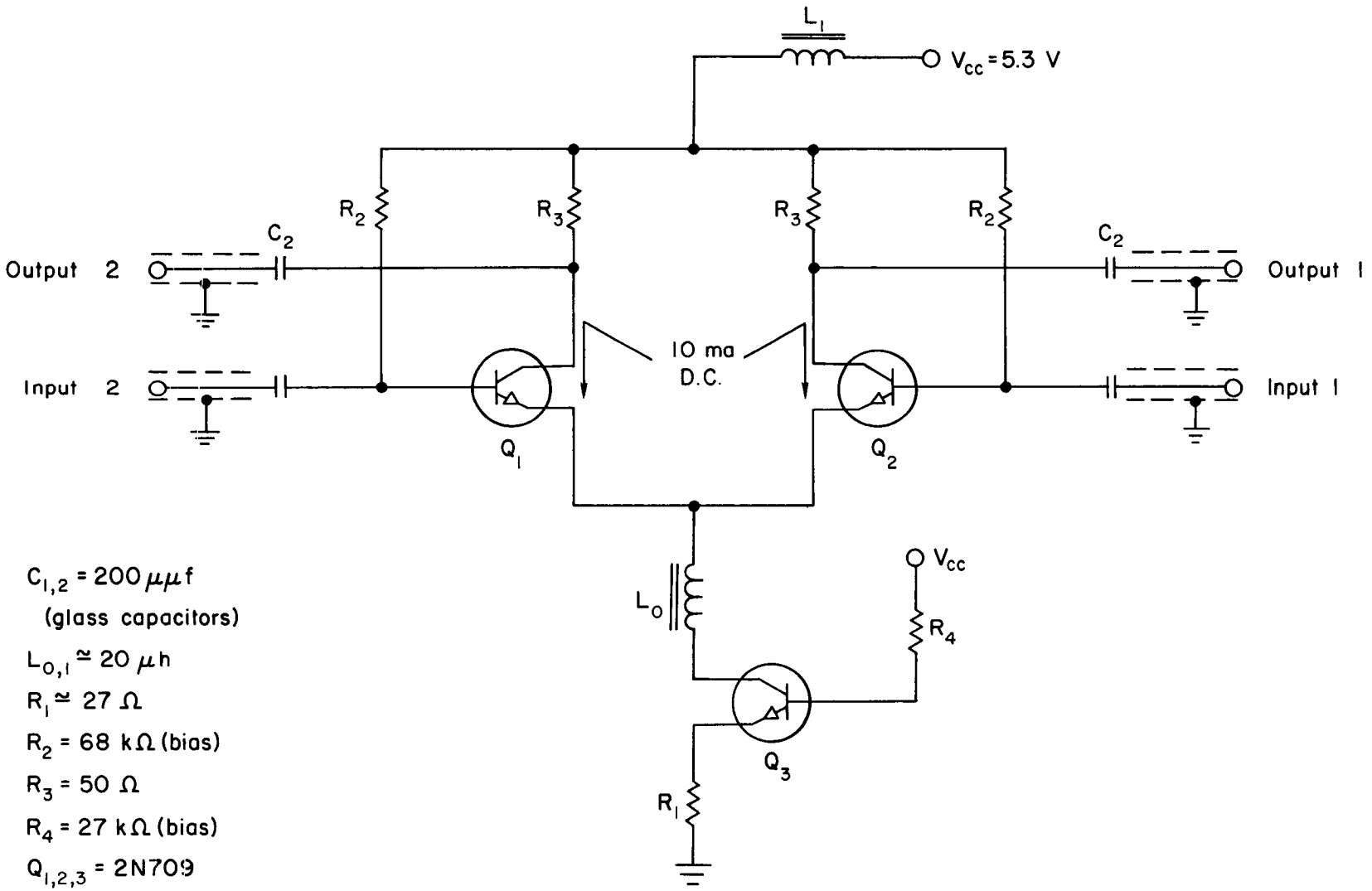

Figure 4.- VHF preamplifier circuit.

NATIONAL AERONAUTICS AND SPACE ADMINISTRATION
AMES RESEARCH CENTER, MOFFETT FIELD, CALIFORNIA

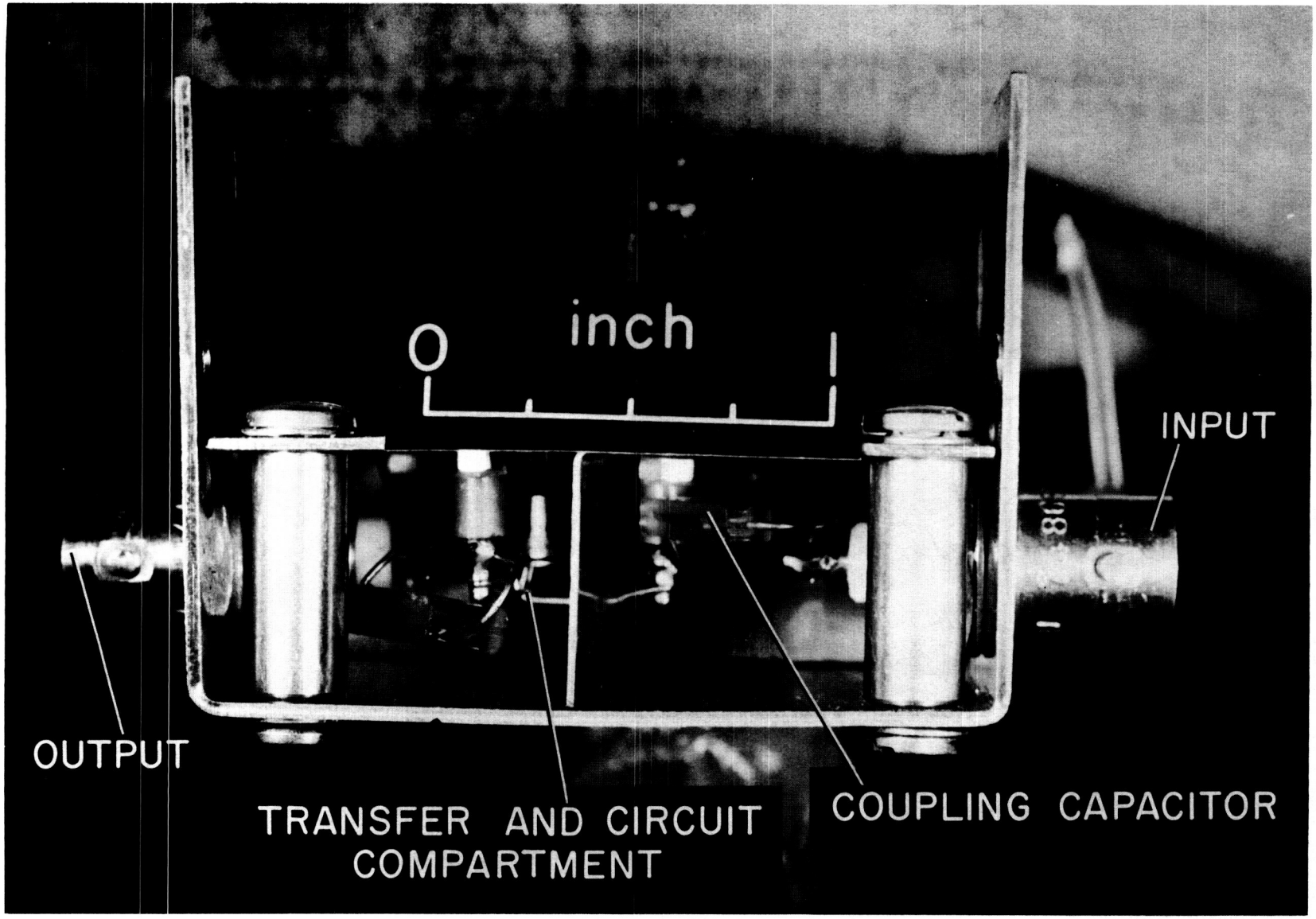

A-32046.1

(a) Input and output compartments.

Figure 5.- Photographs of VHF preamplifier.

NATIONAL AERONAUTICS AND SPACE ADMINISTRATION
AMES RESEARCH CENTER, MOFFETT FIELD, CALIFORNIA

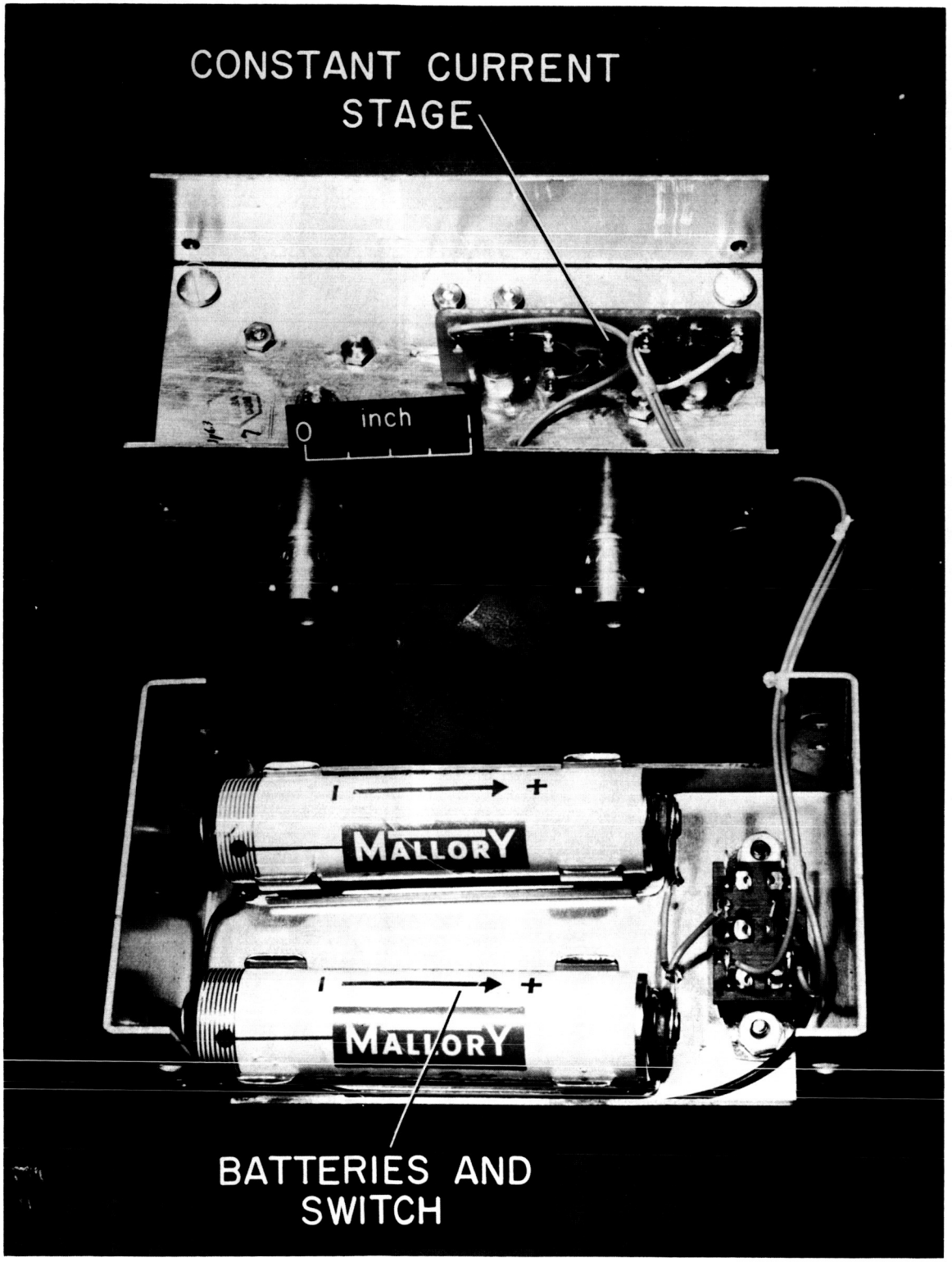

(b) Battery and constant-current stage compartment.

Figure 5.- Concluded.

NATIONAL AERONAUTICS AND SPACE ADMINISTRATION
AMES RESEARCH CENTER, MOFFETT FIELD, CALIFORNIA

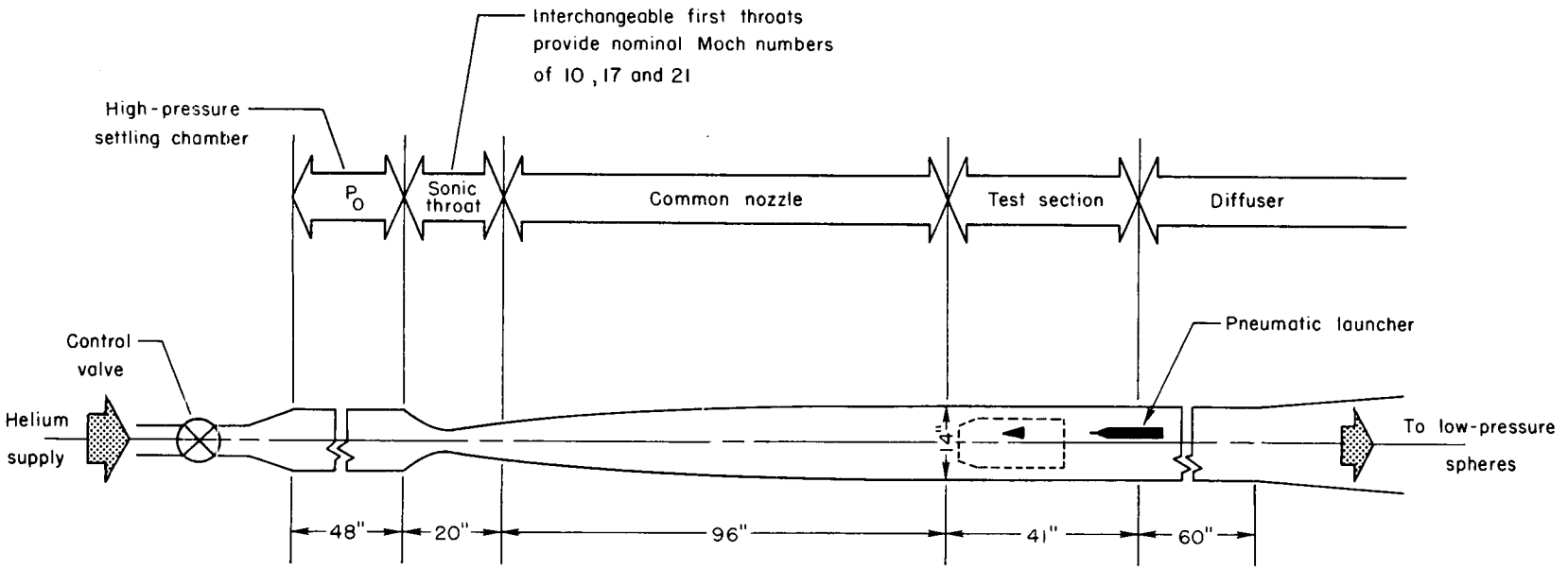

Figure 6.- Schematic of the Ames 14-Inch Helium Tunnel.

NATIONAL AERONAUTICS AND SPACE ADMINISTRATION
AMES RESEARCH CENTER, MOFFETT FIELD, CALIFORNIA

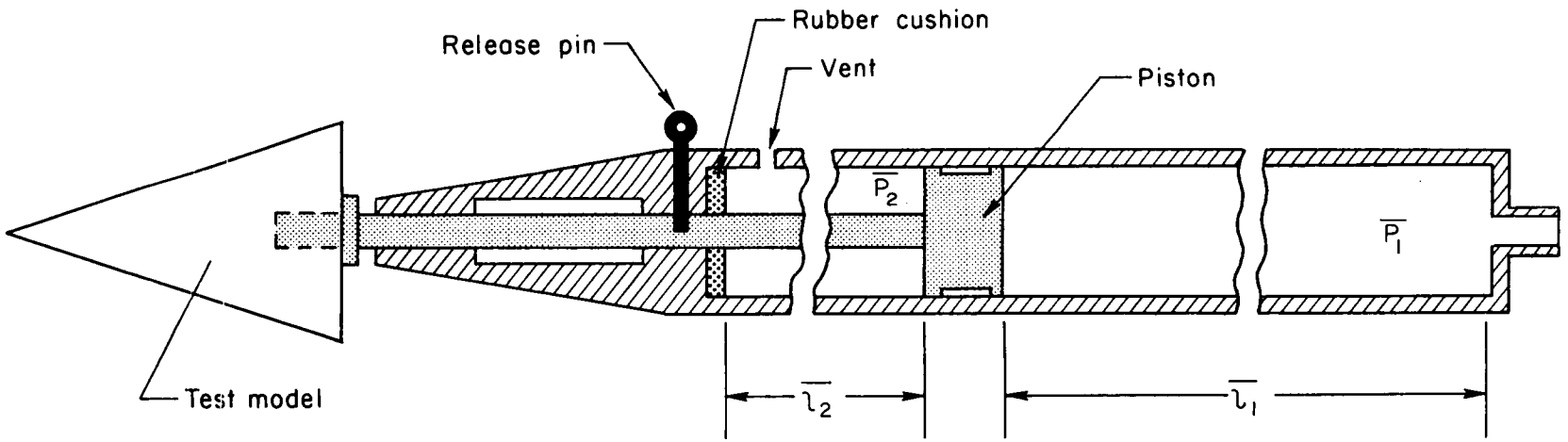

Figure 7.- Schematic of pneumatic model launcher.

NATIONAL AERONAUTICS AND SPACE ADMINISTRATION
AMES RESEARCH CENTER, MOFFETT FIELD, CALIFORNIA

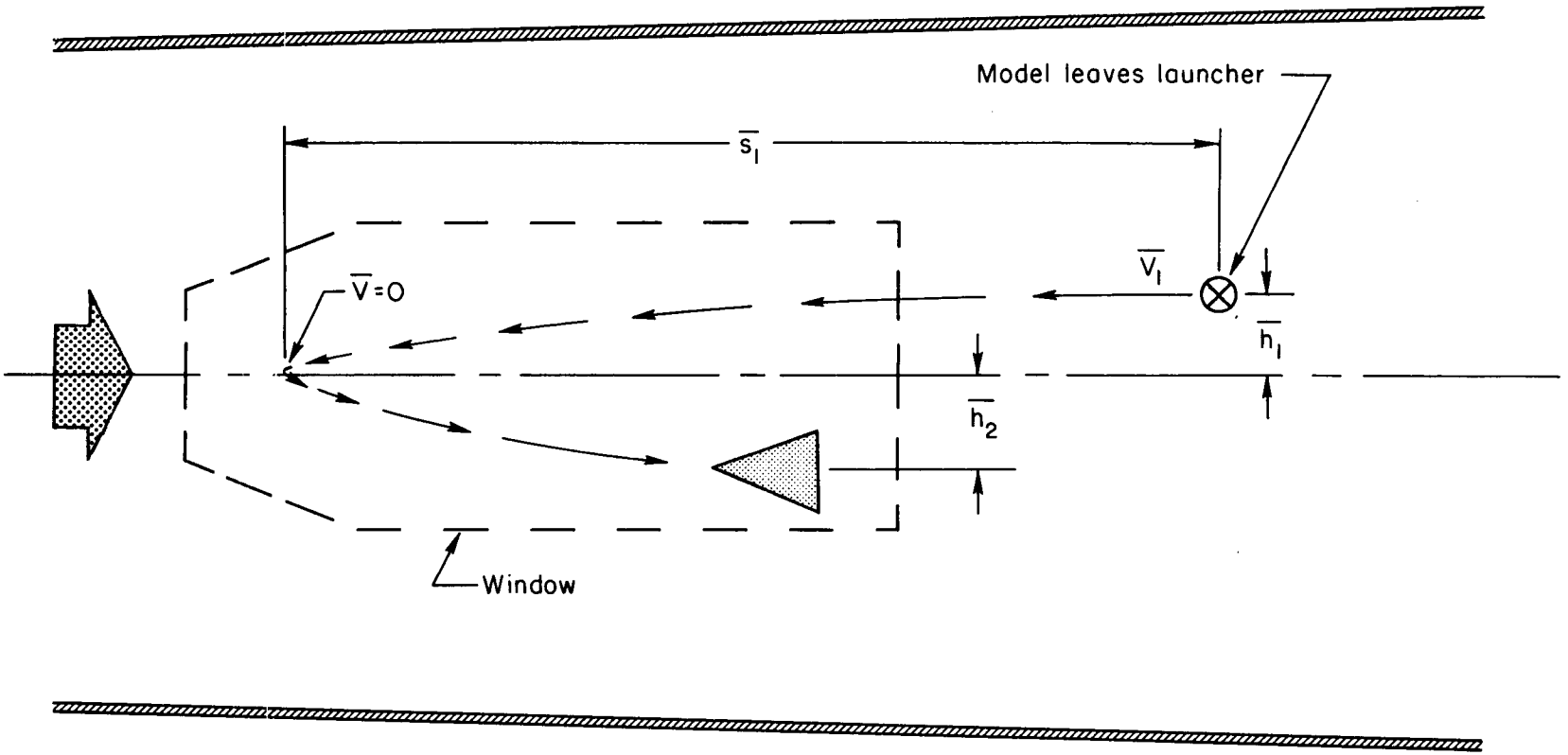

Figure 8.- Free-flight trajectory of model.

NATIONAL AERONAUTICS AND SPACE ADMINISTRATION
AMES RESEARCH CENTER, MOFFETT FIELD, CALIFORNIA

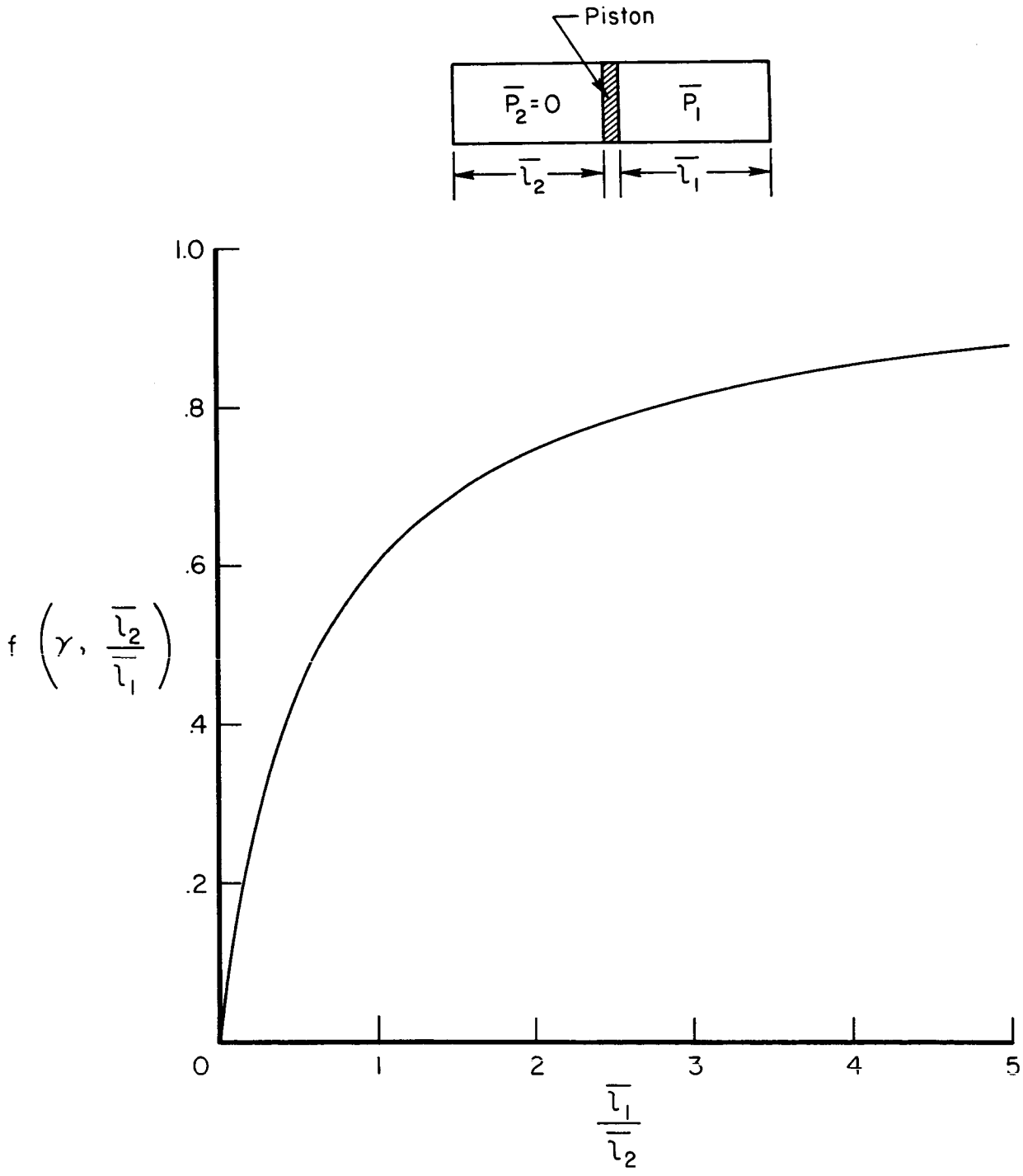

Figure 9.- Variation of $f[\gamma, (\bar{l}_2/\bar{l}_1)]$ with $\bar{l}_1/\bar{l}_2$.

NATIONAL AERONAUTICS AND SPACE ADMINISTRATION
AMES RESEARCH CENTER, MOFFETT FIELD, CALIFORNIA

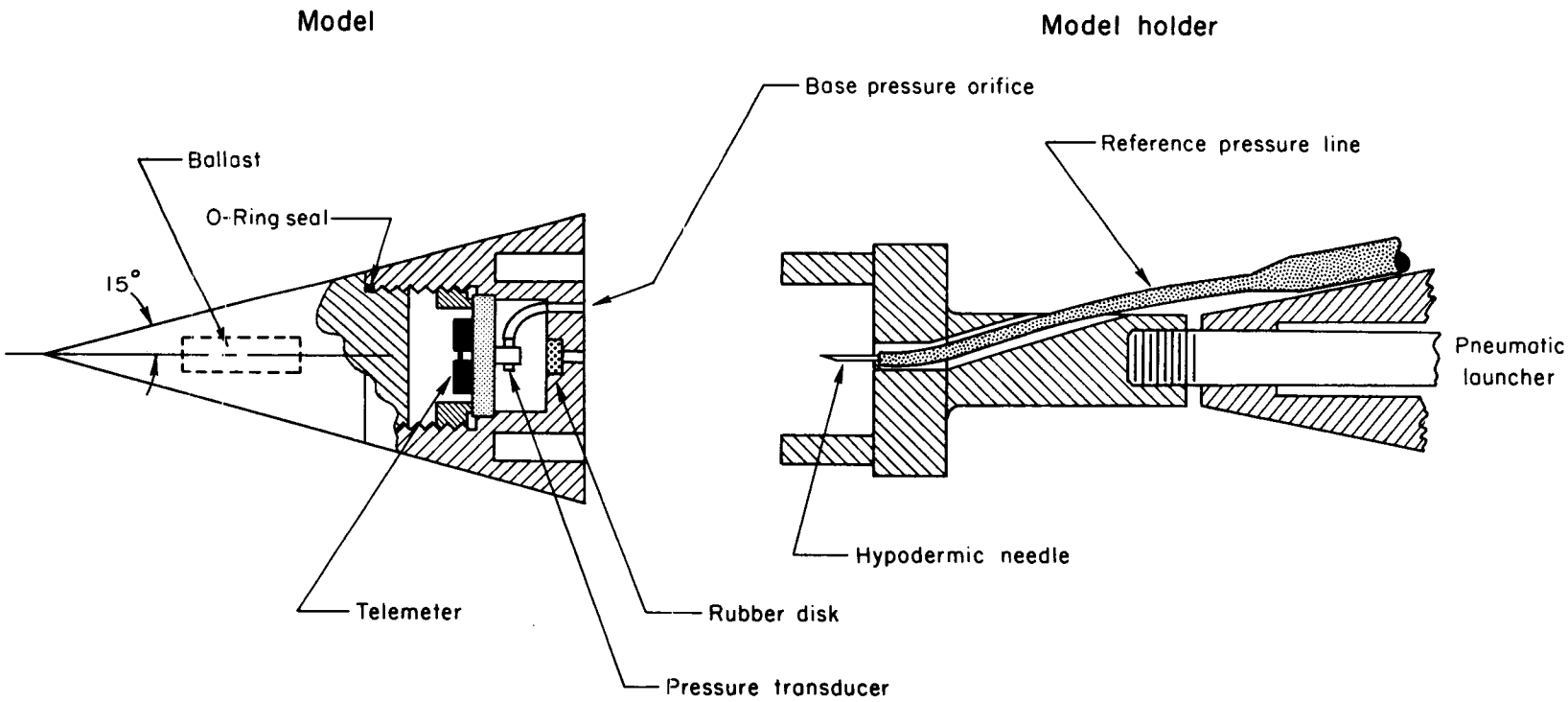

Figure 10.- Details of model and holder.

NATIONAL AERONAUTICS AND SPACE ADMINISTRATION
AMES RESEARCH CENTER, MOFFETT FIELD, CALIFORNIA

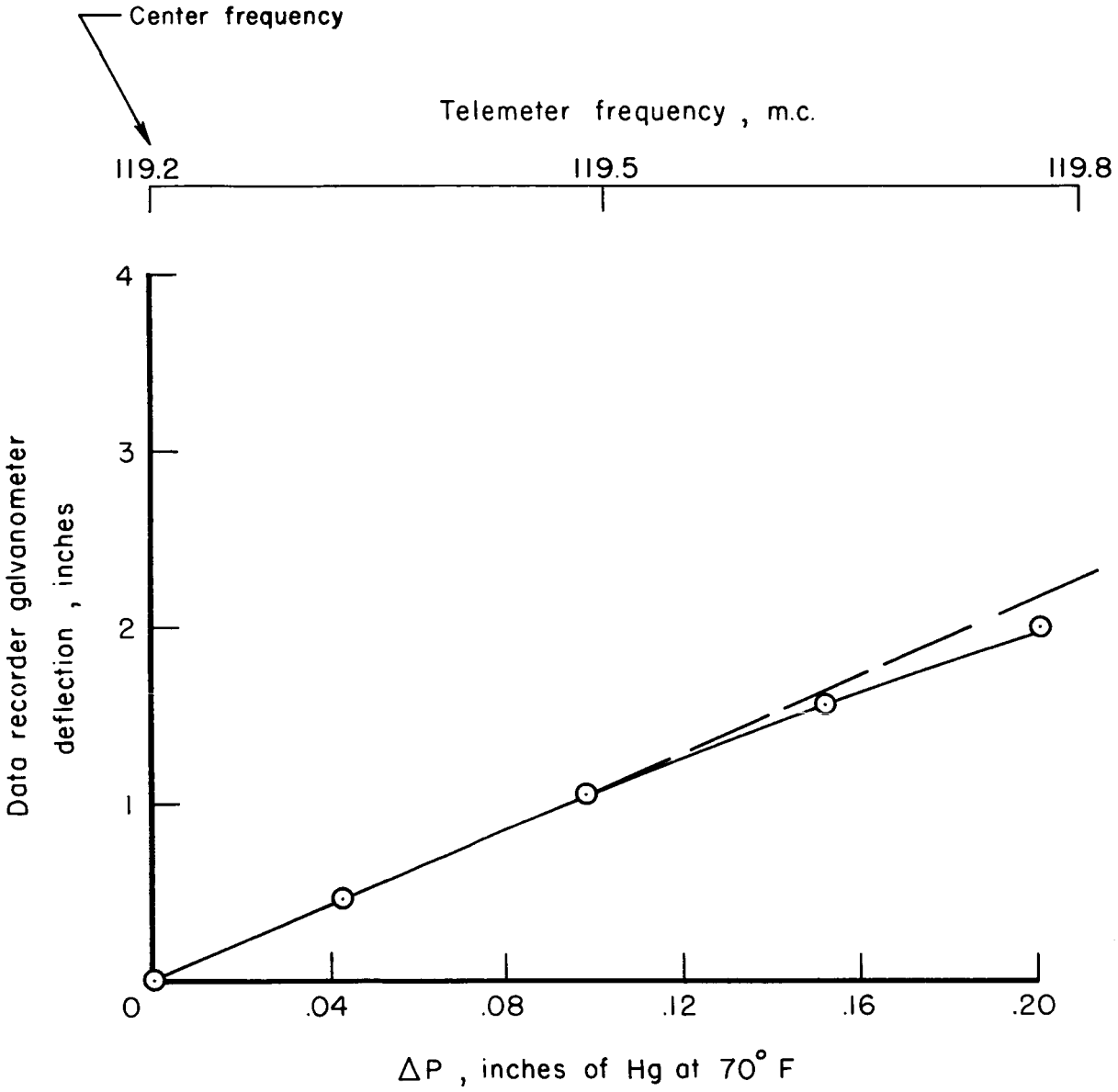

Figure 11.- Calibration of pressure transducer.

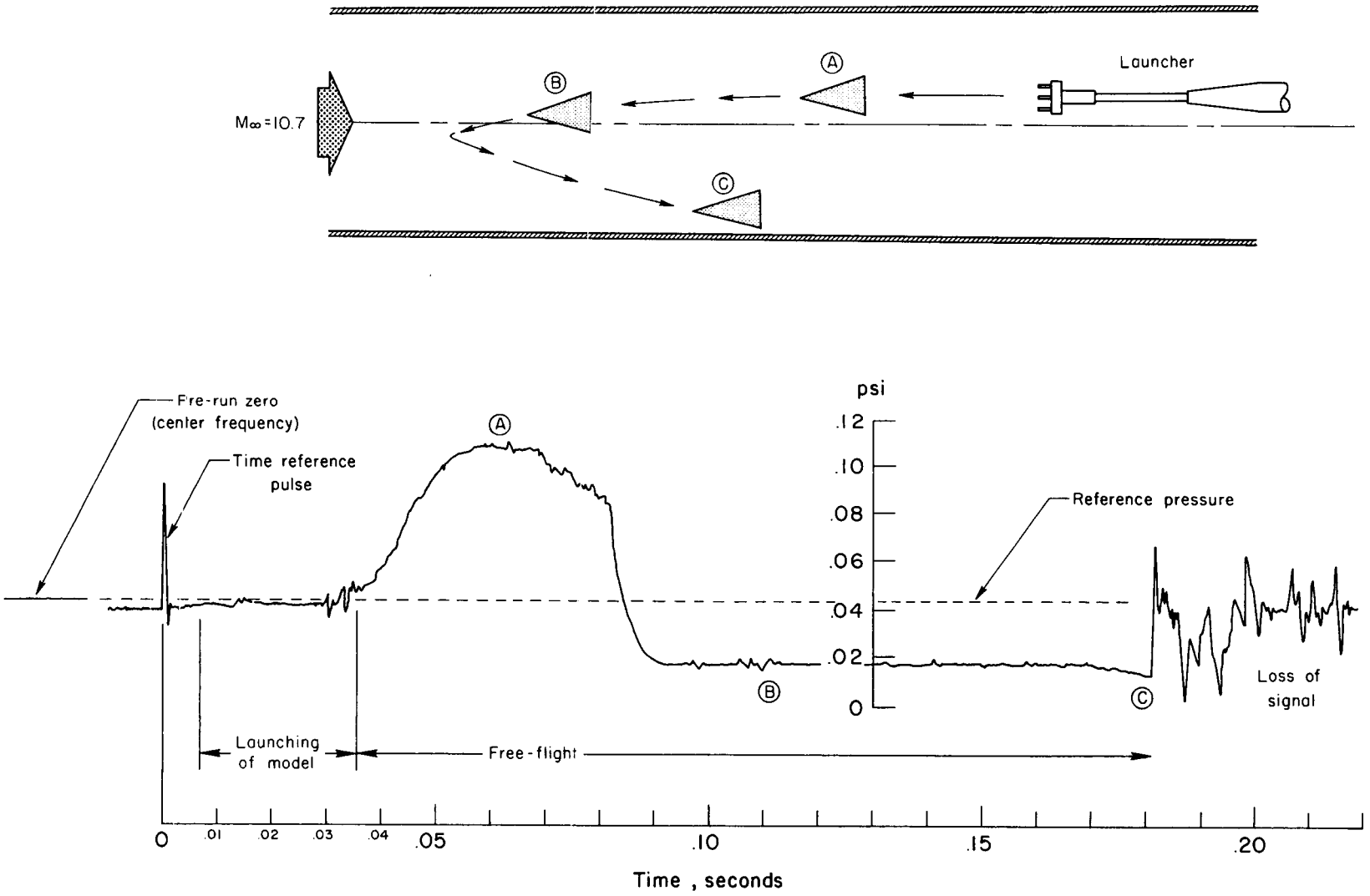

Figure 12.- Data-recorder trace of free-flight base-pressure telemetry.

NATIONAL AERONAUTICS AND SPACE ADMINISTRATION
AMES RESEARCH CENTER, MOFFETT FIELD, CALIFORNIA

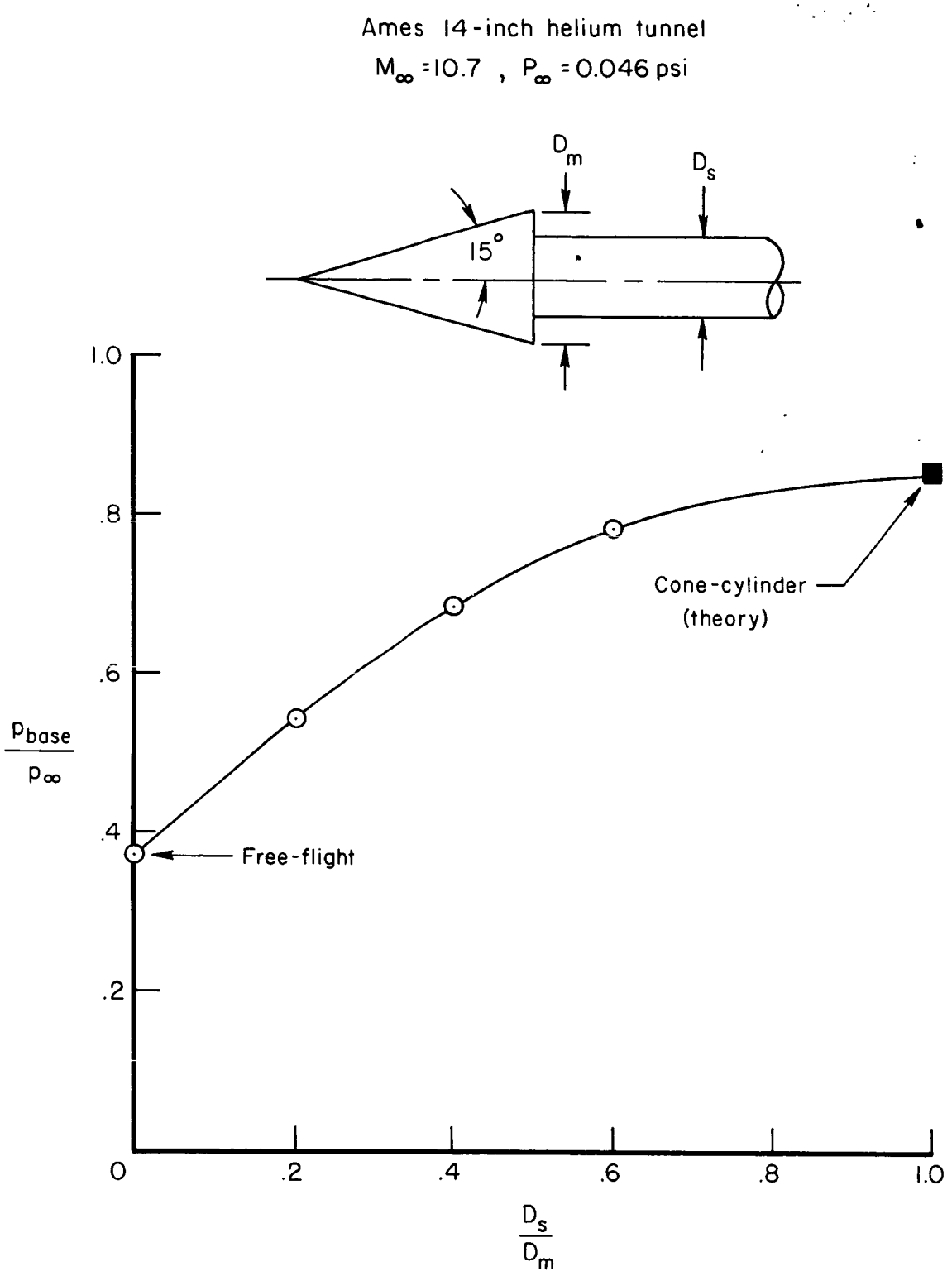

Figure 13.- Effect of sting size on model base pressure.

NATIONAL AERONAUTICS AND SPACE ADMINISTRATION
AMES RESEARCH CENTER, MOFFETT FIELD, CALIFORNIA